



HAL
open science

Mechanism insights in controlling host-guest (de)complexation by thermoresponsive polymer phase transitions

Hui Guo, Gaëlle Le Fer, Thi Nga Tran, Aurélie Malfait, Dominique Hourdet,
Alba Marcellan, François Stoffelbach, Joël Lyskawa, Richard Hoogenboom,
Patrice Woisel

► **To cite this version:**

Hui Guo, Gaëlle Le Fer, Thi Nga Tran, Aurélie Malfait, Dominique Hourdet, et al.. Mechanism insights in controlling host-guest (de)complexation by thermoresponsive polymer phase transitions. *Polymer Chemistry*, 2022, 13 (25), pp.3742-3749. 10.1039/D2PY00219A . hal-03790536

HAL Id: hal-03790536

<https://hal.science/hal-03790536v1>

Submitted on 28 Sep 2022

HAL is a multi-disciplinary open access archive for the deposit and dissemination of scientific research documents, whether they are published or not. The documents may come from teaching and research institutions in France or abroad, or from public or private research centers.

L'archive ouverte pluridisciplinaire **HAL**, est destinée au dépôt et à la diffusion de documents scientifiques de niveau recherche, publiés ou non, émanant des établissements d'enseignement et de recherche français ou étrangers, des laboratoires publics ou privés.

Mechanism insights in controlling host-guest (de)complexation by thermoresponsive polymer phase transitions

Hui Guo,^{*[a],[b]} Gaëlle Le Fer,^[c] Thi Nga Tran,^[b] Aurélie Malfait,^[c] Dominique Hourdet,^[b]

Alba Marcellan,^[b] François Stoffelbach,^{*[d]} Joël Lyskawa,^[c] Richard Hoogenboom,^[e] and

Patrice Woisel^{*[c]}

[a] School of Chemical Engineering and Technology, Sun Yat-sen University, Zhuhai 519082, China

[b] Soft Matter Sciences and Engineering, ESPCI Paris, PSL University, Sorbonne University, CNRS, F-75005 Paris, France

[c] Univ. Lille, CNRS, INRAE, Centrale Lille, UMR 8207 - UMET - Unité Matériaux et Transformations, F-59000 Lille, France

[d] Sorbonne Université, CNRS, Institut Parisien de Chimie Moléculaire, UMR 8232, Equipe Chimie des Polymères, F-75252 Paris Cedex 05, France

[e] Supramolecular Chemistry Group, Centre of Macromolecular Chemistry (CMaC), Department of Organic and Macromolecular Chemistry, Ghent University, Krijgslaan 281 S4-bis, 9000 Ghent, Belgium

Abstract. The combination of (thermo)responsive polymers with supramolecular chemistry recently allowed the development of adaptative materials based on the reversible regulation of host-guest complexation. The properties of these artificial systems rely on their synthetic design, which requires a perfect understanding of the mechanisms triggering the thermo-induced decomplexation. Despite recent progress, the origins of this phenomenon are still not fully understood. To investigate the effect of phase separation mechanism and thermodynamics on the host-guest (de)complexation behavior, different naphthalene-functionalized (guest) thermoresponsive polymers, including lower critical solution temperature (LCST) and upper critical solution temperature (UCST) polymers, were prepared. The host-guest complexation of the polymers with cyclobis(paraquat-*p*-phenylene) (Blue Box) was investigated in water at different temperatures. Host-guest complexation was lost upon heating-induced hydrophobic phase separation of complexed guest-functionalized LCST-polymers, while, in contrast, the host-guest complex was retained upon cooling-induced hydrogen bond-driven phase separation of a complexed guest-functionalized UCST polymer. This comparative analysis showed that the mechanism behind the thermoresponsive polymer phase separation is a key factor that dominates the host-guest (de)complexation.

Introduction

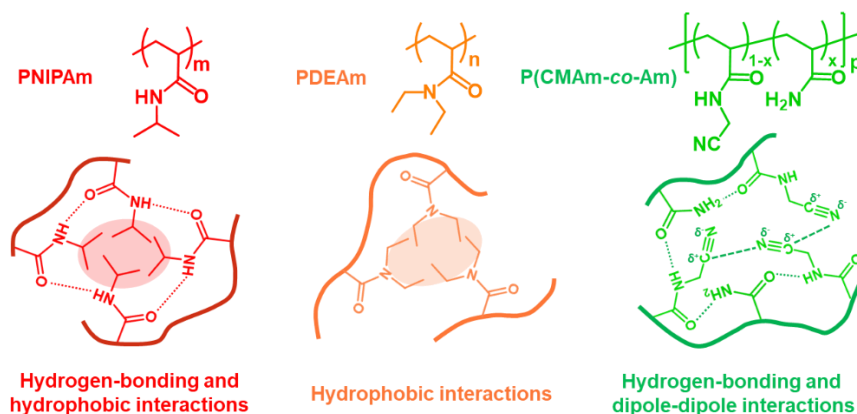
For the last several decades, the concepts of supramolecular chemistry allowed the development of synthetic systems of increasing complexity with bio-inspired properties such as specific recognition,¹ self-assembly behavior² and adaptability.³ Host-guest chemistry is a specific type of molecular recognition that is driven by non-covalent supramolecular interactions. Natural systems have inspired researchers to develop triggerable quasi-mechanical movements of host-guest complexes based on stimuli-responsive recognition between host and guest molecules.⁴ For example, the common electron-deficient macrocyclic host cyclobis(paraquat-*p*-phenylene) (Blue Box, abbreviated as **BBox**) can form colored donor-acceptor complexes with electron-rich guests naphthalene or tetrathiafulvalene derivatives both in organic and aqueous solutions.⁵ Upon triggering the host or guest molecules by oxidation/reduction/protonation, the host-guest complexes can be switched between the complexed (ON) and non-complexed (OFF) states to prompt molecular motion.⁶⁻⁹ While these features endow the **BBox**-based molecular machines with various potential input signals, all of these triggers rely on a chemical change of the host or guest modules themselves. More recently, it has been demonstrated that the reversibility of this host-guest complexation can also indirectly be induced by the phase transition of a responsive polymer linked to the electron-rich guest molecules.¹⁰⁻¹³ For instance, by incorporating the dialkoxynaphthalene guest module at the end of a poly(*N*-isopropylacrylamide) (PNIPAm) chain that shows a lower critical solution temperature (LCST) behavior, the dissociation of its complexes with **BBox** could be triggered by the coil to globule transition of PNIPAm upon heating above its cloud point temperature (T_{cp}). As a result, these host-guest complexes can be easily switched ON and OFF without changing the chemical

properties of the host or guest, which was ascribed to a loss of hydrophobic driving force for host-guest complexation upon dehydration of the polymer.¹² This observed heating-induced decomplexation is an intriguing, but rather specific phenomenon as most other kinds of host-guest complexes attached to a thermoresponsive polymer have been reported to retain in the complexed state upon crossing the cloud point temperature (T_{cp}) (e.g., cyclodextrins,¹⁴⁻¹⁶ pillararene¹⁷ hosts or terpyridine ligands¹⁸). Benefiting from this LCST-induced decomplexation process that is accompanied by the loss of the characteristic color of the donor-acceptor host-guest complex, this reversible temperature-controlled host-guest interaction can serve as an ideal platform for various potential applications, such as targeted molecular release, or thermo-responsive sensors. In previous efforts to further understand this heating-induced decomplexation of **BBox**-complexed **naphthalene** functionalized PNIPAm, we determined that the host-guest complexes remain stable in the collapsed state if the PNIPAm chains are terminated by the host molecule **BBox** and complexed with **naphthalene**.¹⁹ These results indicate that the hydrophilicity of the tetracationic **BBox** also plays a role in the LCST-induced decomplexation as the more hydrophobic **naphthalene** is retained in the collapsed polymer globules. Furthermore, the thermoresponsive polymer was altered to different poly(oligoethylene glycol acrylate)s (POEGAs), revealing that the decomplexation started before the LCST-phase transition temperature, while complete decomplexation only occurred at the LCST phase transition of the polymer.²⁰ In accordance, a fully-hydrophilic polymer did not lead to full decomplexation upon heating.

Limited by the current research on this peculiar heating-induced decomplexation of **naphthalene**-functionalized thermoresponsive polymers complexed with **BBox**, many

questions remain uncovered. For instance, is it universal that the solution phase transition of polymer chains leads to decomplexation of these types of host-guest complexes? And what is the driving force for host-guest dissociation? To further shed light on these fundamental questions, other thermoresponsive polymers, including both LCST and upper critical solution temperature (UCST)-types, have been investigated in this work to complement our knowledge on PNIPAm- and POEGA-based systems. In general, LCST-type polymers have an entropy-driven phase transition based on dehydration of the polymer chains leading to hydrophobic collapse into mesoglobules.²¹ For PNIPAm, the collapsed globules are further held together by intermolecular hydrogen bonding (Scheme 1). Therefore, we have investigated poly(*N,N*-diethylacrylamide) (PDEAm; Scheme 1) as alternative polyacrylamide LCST-polymer where the mesoglobules are only held together by hydrophobic collapse without further intermolecular hydrogen bonding, allowing us to evaluate the effect of this additional hydrogen bonding on the host-guest decomplexation. Note that this could not be done with the previously reported POEGA systems as these retain much more water in the collapsed phase. The reversed UCST transition is an enthalpically driven phase transition through stronger polymer-polymer attraction at lower temperatures.²² Here, we chose to investigate poly(*N*-cyanomethylacrylamide-*co*-acrylamide) (P(CMAm-*co*-Am)) as a UCST-copolymer, which phase separates at low temperature thanks to intermolecular hydrogen-bonding and dipole-dipole interactions (Scheme 1).²³ Since the LCST phase transition of PNIPAm above T_{cp} results in complete dissociation of **BBox** based complexes, investigating whether **BBox** complexes of **naphthalene**-functionalized PDEAm and P(CMAm-*co*-Am) can also be disrupted by temperature-induced coil to globule transitions will allow us to evaluate the importance and

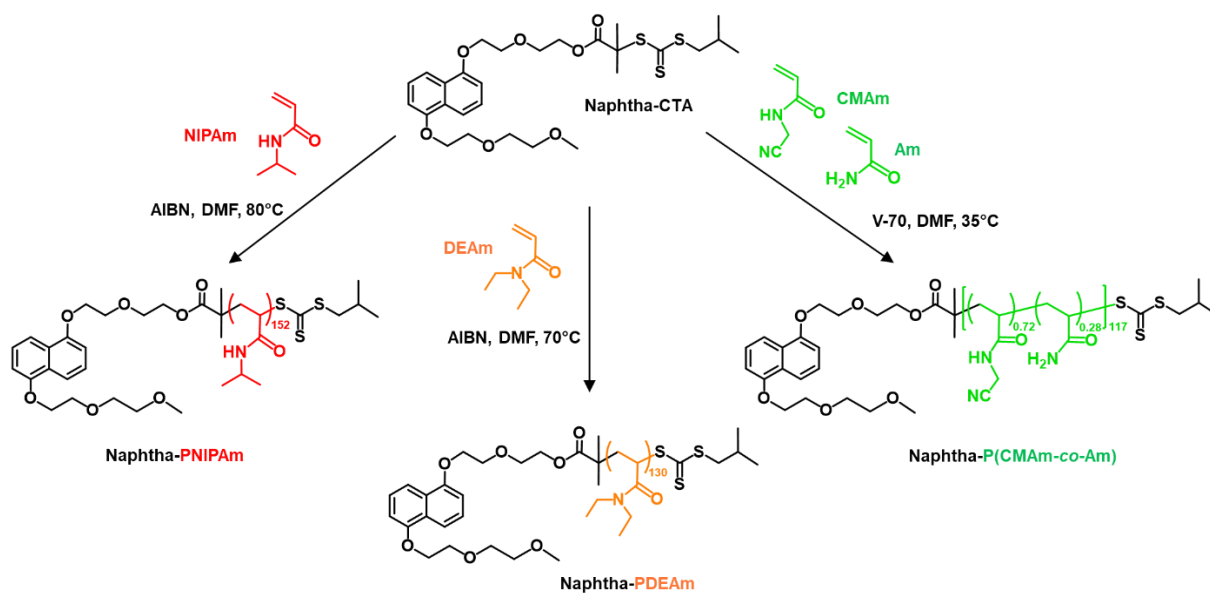
contribution of the different factors, such as interpolymer hydrogen bonding and phase-separation thermodynamics, on the polymer phase transition induced host-guest decomplexation.



Scheme 1. Thermoresponsive polymers investigated in this work (top) and the physical interactions that dominate in the collapsed mesoglobule state (bottom).

Results and discussion

PNIPAm and PDEAm polymers, as well as a P(CMAM-*co*-Am) copolymer end-functionalized by a naphthalene group (**Naphtha**), were prepared by Reversible addition-fragmentation chain-transfer (RAFT) polymerization using a Naphtha-functionalized RAFT agent (**Naphtha-CTA**) (Scheme 2). As PCMAm homopolymers display high T_{cp} ($> 75^{\circ}\text{C}$ for $\overline{DP}_n > 55$),²³ a copolymer P(CMAM-*co*-Am) containing 28 mol% of acrylamide was synthesized to target a lower T_{cp} . Table 1 summarizes the experimental conditions for the RAFT-mediated (co)polymerizations of NIPAm, DEAm, and CMAM/Am and the molecular characteristics of the obtained Naphtha-functionalized (co)polymers.



Scheme 2. Synthetic routes for **Naphtha-PNIPAm**, **Naphtha-PDEAm** and **Naphtha-P(CMAM-co-Am)**.

Table 1. Experimental conditions and molecular characteristics of the obtained polymers for the RAFT-mediated (co)polymerizations of NIPAm, DEAm, and CMAM/Am performed in DMF.

Polymer	[M] ₀ : [CTA] ₀ : [AIBN] ₀	Temp. (°C)	Time (min)	Conv. (%) ^a	\overline{DP}_n ¹ H NMR ^a	\overline{M}_n ¹ H NMR (kg·mol ⁻¹) ^a	\overline{M}_n SEC (kg·mol ⁻¹) ^b	\mathcal{D}^b
Naphtha-PNIPAm	160:1:0.25	80	120	94	152	17.8	6.6	1.37
Naphtha-PDEAm	140:1:0.24	70	180	93	130	17.1	9.8	1.24
Copolymer	[CMAM] ₀ : [Am] ₀ : [CTA] ₀ : [V-70] ₀	Temp. (°C)	Time (min)	Conv. CMAM/Am (%) ^a	\overline{DP}_n CMAM/Am ¹ H NMR ^a	\overline{M}_n ¹ H NMR (kg·mol ⁻¹) ^a	\overline{M}_n SEC (kg·mol ⁻¹) ^b	\mathcal{D}^b
Naphtha-P(CMAM-co-Am)	102:44:1:0.5	35	180	65/59	83/33	12.1	14.2	1.32

^a determined by ¹H NMR in D₂O for Naphtha-PNIPAm and Naphtha-PDEAm or DMSO-d₆ for Naphtha-P(CMAM-co-Am); ^b SEC in THF, RI detector, PS standards for Naphtha-PNIPAm and Naphtha-PDEAm and SEC in DMF, RI detector, PMMA standards for Naphtha-P(CMAM-co-Am).

¹H NMR spectra recorded on (co)polymers (in D₂O for **Naphtha-PNIPAm** and **Naphtha-PDEAm**, or in DMSO-d₆ for **Naphtha-P(CMAM-co-Am)**) confirmed the connection of the

naphthalene group to polymer chains with the presence of characteristic resonances of H_{2/6} (7.0 ppm), H_{3/7} (7.4 ppm) and H_{4/8} (7.7 ppm) protons located on the naphthalene moiety (Fig. S1, S2 and S3). Comparison of integrals of aromatic protons with those of polymer backbones allowed the estimation of the different \overline{DP}_n values that are 152 for **Naphtha-PNIPAm**, 130 for **Naphtha-PDEAm**, and 83/33 for CMAm/Am repetitive units in **Naphtha-P(CMAm-co-Am)**. SEC analyses also indicated that the (co)polymers had monomodal and relatively low dispersity values, in between 1.2 and 1.4 (Fig. S4). After confirming the structure and composition of the (co)polymers, we next investigated their binding properties towards **BBox** (Fig. 1). The addition of 1 equivalent of **BBox** to a solution of the (co)polymers in water in their soluble state (*i.e.*; $T < T_{cp}$ and $T > T_{cp}$ for LCST- and UCST-type (co)polymers, respectively) revealed the appearance of the characteristic purple color of the host-guest complexes between **Naphthalene** and **BBox** (see pictures in Fig. 1). Moreover, UV-vis spectroscopy of solutions of the (co)polymers without and with **BBox** showed the appearance of the characteristic absorption band centered around 500 nm corresponding to the **BBox/naphthalene** complexes (Fig. 1). Based on these results, it can be concluded that all three (co)polymers are capable of forming host-guest complexes with **BBox**.

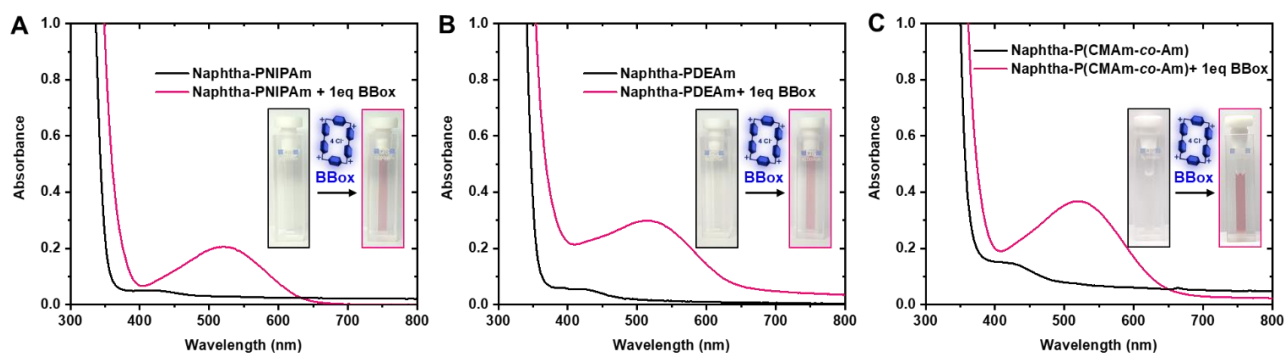


Fig. 1. UV-visible spectra of **Naphtha-(co)polymers** in their soluble state in pure water at 10 mg·mL⁻¹ and pictures of the samples without and with 1 equivalent of **BBox**. A) **Naphtha-PNIPAm** at 20 °C, B)

Naphtha-PDEAm at 20 °C and C) **Naphtha-P(CMAM-co-Am)** at 65 °C.

The ability of the polymers to form supramolecular host-guest complexes with **BBox** in water was also evaluated by isothermal titration calorimetry (ITC), which revealed the formation of 1:1 host inclusion complexes with strong association constants in the order of $10^4 - 10^5 \text{ M}^{-1}$: $K_{a(A)} = (2.76 \pm 0.55) \times 10^5 \text{ M}^{-1}$ for **Naphtha-PNIPAm**, $K_{a(B)} = (4.16 \pm 0.36) \times 10^4 \text{ M}^{-1}$ for **Naphtha-PDEAm**, and $K_{a(C)} = (1.53 \pm 0.06) \times 10^4 \text{ M}^{-1}$ for **Naphtha-P(CMAM-co-Am)** (Fig. S5). These K_a values are in line with the previously reported value for Naphtha-PNIPAM¹² and slightly higher than the values reported for Naphtha-POEGAs, indicating a minor influence of the polymer structure on the K_a .²⁰ Finally, the host-guest complexation between **BBox** and the Naphtha-functionalized (co)polymers was investigated by ¹H NMR spectroscopy in D₂O in their soluble state (*i.e.*; $T < T_{cp}$ and $T > T_{cp}$ for LCST- and UCST-type (co)polymers, respectively). **Fig. 2** presents the partial ¹H NMR spectra of **Naphtha-PNIPAm** (A) as an example of uncomplexed Naphtha-functionalized (co)polymers, complexed **Naphtha-PNIPAm** (B), complexed **Naphtha-PDEAm** (C), complexed **Naphtha-P(CMAM-co-Am)**, (D) and **BBox** alone (E). Whatever the nature of the thermoresponsive (co)polymers, broadening and shifts in resonances of protons from the **BBox** host (H_α , H_β , and H_{ph}) and the **Naphtha** moiety ($H_{2/6}$, $H_{3/7}$ and $H_{4/8}$) were observed indicative of complexation. For both complexed LCST-type polymers (Fig. 2.B and 2.C), characterized at 20 °C, the shift of the characteristic signals upon complexation were similar to those previously reported in the same conditions:¹² $\Delta H_\alpha \approx -0.2 \text{ ppm}$, $\Delta H_\beta \approx -0.8 \text{ ppm}$, $\Delta H_{ph} \approx +0.3 \text{ ppm}$, $\Delta H_{2/6} \approx -0.85 \text{ ppm}$ and $\Delta H_{3/7} \approx -1.35 \text{ ppm}$. The UCST-type polymer, before (Fig. S6) and after complexation (Fig. 2.D), was characterized in D₂O at 90 °C. As a result of the higher temperature, the shift and shape of the characteristic

signals for the host-guest complex were significantly different, but still in agreement with the formation of host-guest complexes after the addition of **BBox**.

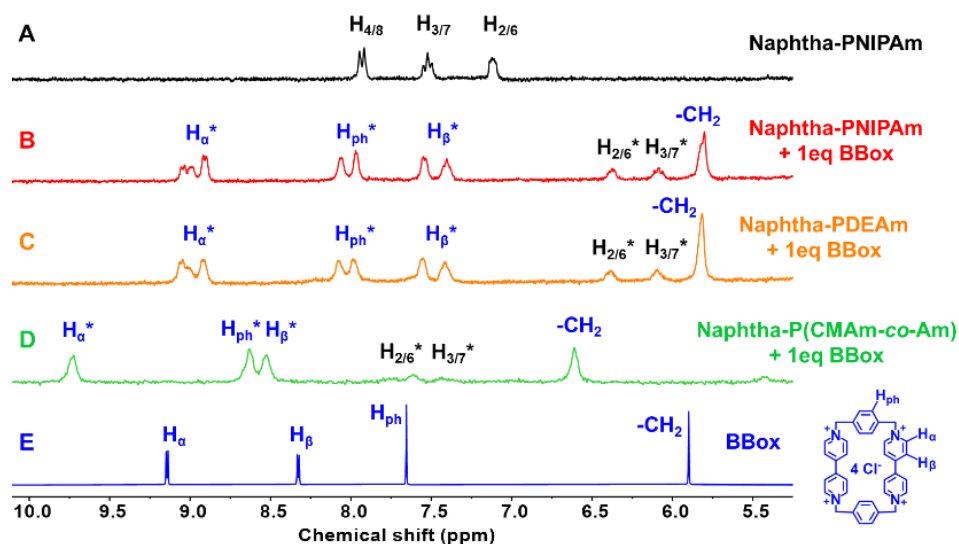


Fig. 2. Partial ^1H NMR spectra in D_2O of A) **Naphtha-PNIPAm** polymer at 20°C , B) **Naphtha-PNIPAm** polymer with 1 eq of **BBox** at 20°C , C) **Naphtha-PDEAm** polymer with 1 eq of **BBox** at 20°C , D) **Naphtha-P(CMAm-co-Am)** with 1 eq of **BBox** at 90°C , E) **BBox** at 20°C . The protons H^* denote complexed protons from naphthalene moieties and **BBox**.

After confirming that all thermoresponsive (co)polymers could form host-guest complexes with **BBox**, we studied the effect of the **BBox** and the host-guest complexation on the phase transitions of the LCST-type and UCST-type (co)polymers (Fig. 3). As previously reported for the **Naphtha-PNIPAm** polymer, the addition of the tetracationic **BBox** led to a slight increase in hydrophilicity and consequently to a 1°C rise in the T_{cp} for both heating and cooling cycles (Fig. 3.A).¹² A similar phenomenon was observed for **Naphtha-PDEAm** with an increase of about 2°C in the T_{cp} (Fig. 3.B). It is also evident that the absence of the intermolecular hydrogen bonding in the PDEAm leads to significantly less hysteresis between heating and cooling cycles compared to PNIPAm. However, in both cases the relatively large hysteresis observed for the LCST polymers with and without **BBox** arises from a phase transition based on dehydration of

the macromolecular chains leading to collapsed hydrophobic mesoglobules, which are more difficult to hydrate and resolubilize upon cooling. For **Naphtha-P(CMAm-co-Am)**, a typical UCST-type thermoresponsive behavior was observed with a sharp transition around $T_{cp} = 57^\circ$. However, the addition of **BBox** and host-guest complexation induced a significant decrease in T_{cp} of 12 °C (Fig. 3.C) due to the increase in hydrophilicity of the complexed system that facilitates polymer hydration and hence dissolution. The very narrow hysteresis observed for this UCST copolymer with and without BBox, in contrast to the LCST polymers, indicates that the collapsed macromolecular chains remain partially hydrated and, consequently, are more easily resolubilized upon heating.

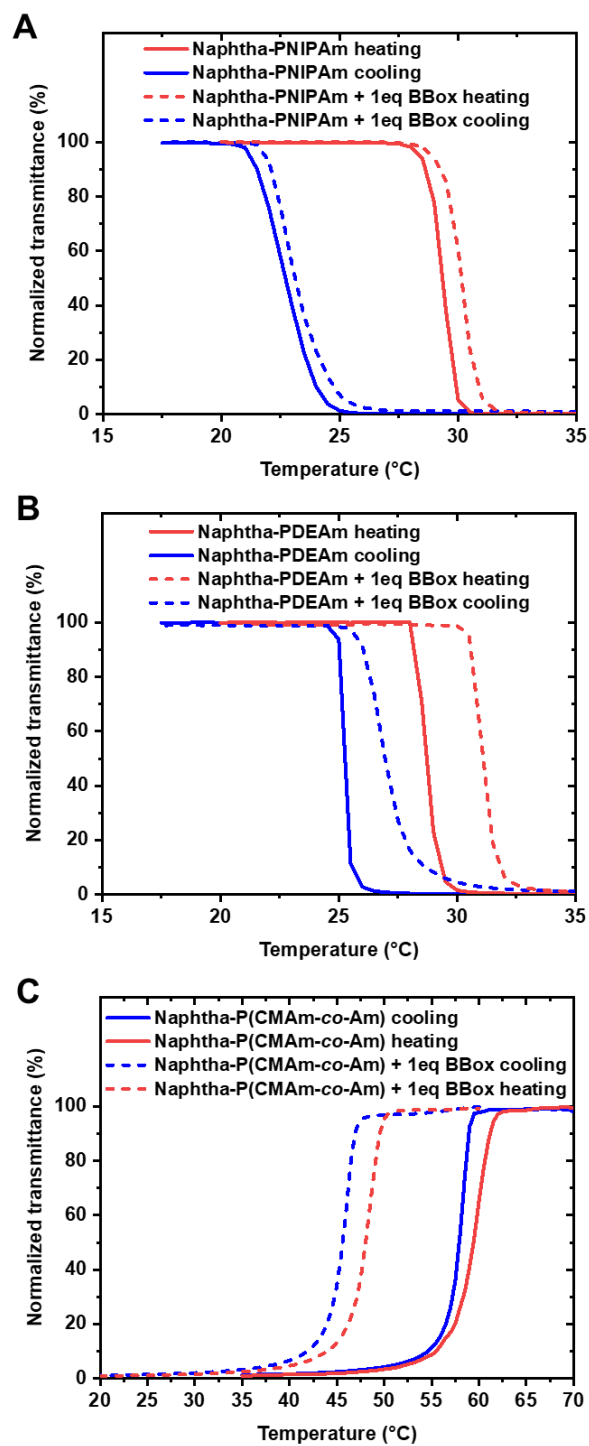


Fig. 3. Turbidity assay in pure water at $10 \text{ mg}\cdot\text{mL}^{-1}$. A) Evolution of normalized transmittance (%) in function of temperature for solutions of **Naphtha-PNIPAm** without and with 1 equivalent of **BBox**, B) Evolution of normalized transmittance (%) in function of temperature for solutions of **Naphtha-PDEAm** without and with 1 equivalent of **BBox**, C) Evolution of normalized transmittance (%) in function of temperature for solutions of **Naphtha-P(CMAm-co-Am)** without and with 1 equivalent of **BBox**.

Then, we investigated the effect of the polymer phase transition on the host-guest complexation state (Fig. 4). Heating **Naphtha-PNIPAm** and **Naphtha-PDEAm** polymers that were complexed with **BBox** above their T_{cp} , resulted in the formation of an opaque white precipitate, indicating the decomplexation during the polymer phase transition (Fig. 4.A and 4.B). In contrast, the purple color of the host-guest complex remained upon cooling of the complexed **Naphtha-P(CMAm-co-Am)** below its T_{cp} (Fig. 4.C). The polymer concentration had no effect on the phase separation mechanisms that induce, or not induce, the decomplexation of the **BBox/naphthalene** host-guest complex since the same phenomena were observed from 5 to 20 $\text{mg}\cdot\text{mL}^{-1}$ (Fig. S7). This preliminary visual test clearly showed that the host-guest association state of thermoresponsive polymers is strongly influenced by the mechanism of the temperature-induced phase transition (LCST versus UCST).

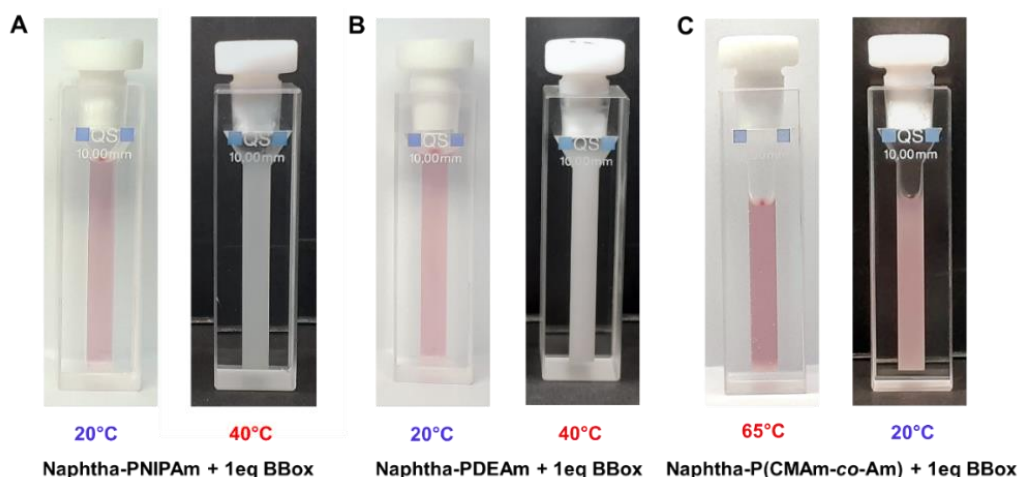


Fig. 4. Photographs of A) **Naphtha-PNIPAm**, B) **Naphtha-PDEAm** and C) **Naphtha-P(CMAm-co-Am)** in pure water at $10 \text{ mg}\cdot\text{mL}^{-1}$ with 1 equivalent of **BBox** at different temperatures.

More solid evidence for the control over the host-guest complexation was provided by ^1H NMR spectroscopy investigations at different temperatures (Fig. 5 and Fig. S8). Both complexed **Naphtha-PNIPAm** and **Naphtha-PDEAm** underwent a coil-to-globule transition during

temperature increase due to partial dehydration, resulting in almost complete disappearance of resonance signals from the thermoresponsive polymer backbone in ^1H NMR spectra. Simultaneously, the characteristic signals from the host-guest complex of **BBox** (ΔH_α^* , ΔH_β^* , ΔH_{Ph}^*) and the **naphthalene** moieties ($\Delta H_{2/6}^*$ and $\Delta H_{3/7}^*$) completely vanished, while signal of the uncomplexed **BBox** appeared as a direct evidence of the dissociation of the **BBox/Naphtha** complexes (Fig. 5.B and Fig. 5.C). In contrast, despite that the ^1H NMR signals from the Naphtha-P(CMAm-*co*-Am) backbone decreased significantly with decreasing temperature due to collapse of the polymer (Fig. S8.D), the signals of the terminal naphthalene group and the **BBox** remained nearly unaltered, implying that the phase transition of the polymer chains did not induce decomplexation of **BBox/Naphtha** host-guest complexes when attached to the P(CMAm-*co*-Am) UCST thermoresponsive polymer.

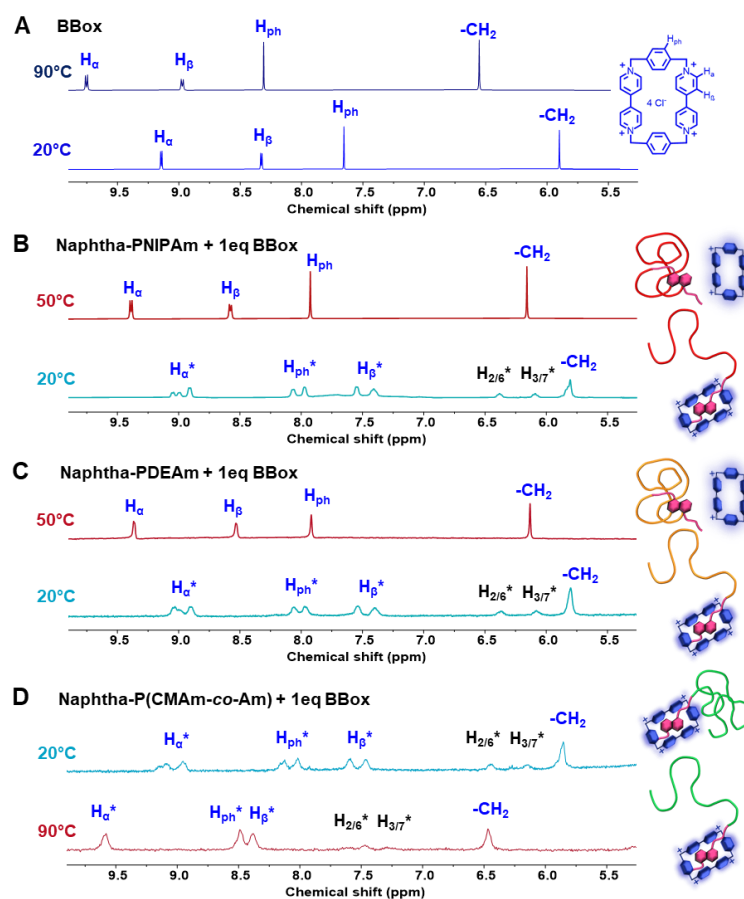


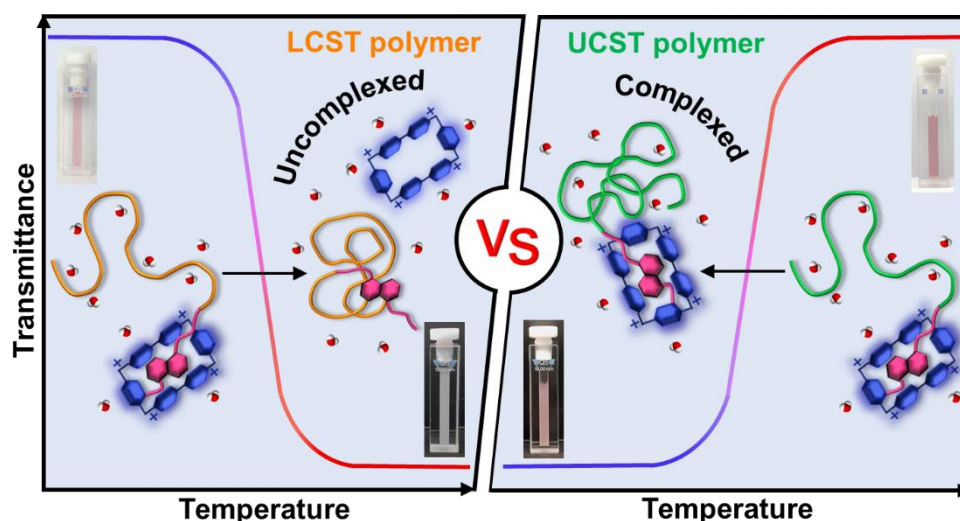
Fig. 5. Partial ^1H NMR spectra in D_2O of A) **BBox** alone at 20 and 90 °C (for comparison), B) **Naphtha-PNIPAm** polymer with 1 equivalent of **BBox** at 20 °C ($< T_{\text{cp}}$) and 50 °C ($> T_{\text{cp}}$), C) **Naphtha-PDEAm** polymer with 1 equivalent of **BBox** at 20 °C ($< T_{\text{cp}}$) and 50 °C ($> T_{\text{cp}}$), D) **Naphtha-P(CMAM-co-Am)** with 1 equivalent of **BBox** at 90 °C ($> T_{\text{cp}}$) and 20 °C ($< T_{\text{cp}}$). The protons H^* denote complexed protons from naphthalene moieties and **BBox**.

These results demonstrate that the phase transition mechanism of the responsive polymers is a critical factor that controls the host-guest association between the electron-deficient **BBox** and the electron-rich naphthalene moieties. When the phase separation is mainly driven by hydrophobic interactions, *i.e.*, LCST-transition of **Naphtha-PNIPAm** and **Naphtha-PDEAm**, the host-guest complex totally dissociates upon the hydrophobic collapse of the polymer, regardless of whether or not additional intermolecular hydrogen bonds occur in the collapsed state. Conversely, the UCST phase separation of **Naphtha-P(CMAM-co-Am)** induced by

hydrogen-bonding and dipole-dipole interactions does not break the assemblies between **BBox** and naphthalene. These antagonistic properties can be explained on the basis of the underlying mechanisms of the polymer phase separation. In the case of the LCST-type phase transition of poly(*N*-alkylacrylamide) derivatives, induced by hydrophobic interactions, the relatively hydrophobic naphthalene terminal group can dissociate from the **BBox** and interacts within the dehydrated mesoglobule polymer, while the hydrophilic **BBox** and its counterions are released from the hydrophobic environment into the aqueous environment. On the contrary, in the case of the hydrophilic **Naphtha-P(CMAm-co-Am)** complexed with **BBox**, the chain collapses under cooling due to enhanced interchain interactions but remains relatively more hydrated, swollen, during this process as attested by ¹H NMR at low temperature still showing the signals from the polymer backbone (Fig. S8.D). As a result, the tetracationic **BBox** and its counterions can still be accommodated in this aqueous environment. Furthermore, the interactions of the hydrophobic naphthalene end-group with this polar environment would also be thermodynamically unfavorable, thus favoring the complexed state during the collapse of the polymer. Accordingly, the reason that the collapse of the previously reported **BBox**-functionalized PNIPAm cannot induce dissociation of its host-guest complex with free naphthalene upon heating-induced collapse can also be easily comprehended.¹⁹ Indeed, in this case, the **BBox** is covalently attached to the collapsed mesoglobules and there is no driving force to release naphthalene as it remains preferentially complexed in the hydrophobic environment inside the **BBox**.

Conclusion

In this work, we provided insights into the effect of the phase separation mechanism of Naphtha-functionalized thermoresponsive polymers revealing that the hydrophobic interactions involved in phase separation of LCST polymers are the critical factor inducing the release of the **BBox** from the **BBox/naphthalene** complexes. In contrast, the phase separation of a Naphtha-functionalized UCST polymer upon cooling did not induce the release of the **BBox**, ascribed to the higher hydrophilicity of the collapsed polymer chains below the UCST (Scheme 3).



Scheme 3. Representation of the **BBox/Naphtha** host-guest decomplexation during phase separation upon heating for the LCST polymers (left) and the retention of the **BBox/Naphtha** host-guest complexes during phase separation upon cooling for the UCST copolymer (right).

Interestingly, since the decomplexation also relies on the incompatibility between the tetracationic hydrophilic **BBox** and the hydrophobicity of the macromolecular chains in their globular state, we hypothesize that a similar phenomenon can also be induced by using other types of host or guest molecules in a charged form. More importantly, this thorough understanding of the mechanism responsible for the thermo-induced guest-host decomplexation paves the way toward the future design of systems of increasing structural complexity with

dedicated functions, such as smart delivery of substances, responsive biomimetic soft materials with molecular communication capability, or tunable recognition between specific molecules.

Acknowledgments

The authors would like to thank Dr. Gaëlle Pembouong for her help in performing ITC and SEC experiments.

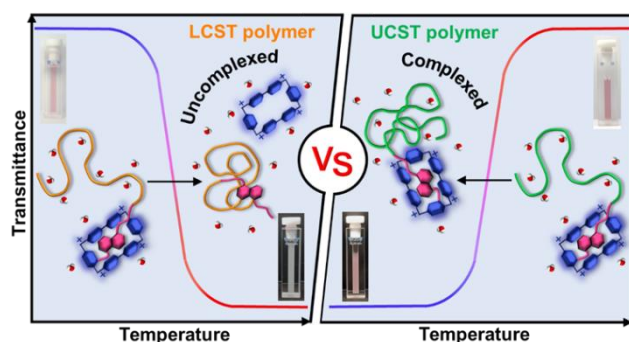
References

1. J.-M. Lehn, *Pure applied chemistry*, 1994, **66**, 1961-1966.
2. S. I. Stupp and L. C. Palmer, *Chemistry of Materials*, 2014, **26**, 507-518.
3. H. Shigemitsu, T. Fujisaku, W. Tanaka, R. Kubota, S. Minami, K. Urayama and I. Hamachi, *Nature nanotechnology*, 2018, **13**, 165-172.
4. D.-H. Qu, Q.-C. Wang, Q.-W. Zhang, X. Ma and H. Tian, *Chemical reviews*, 2015, **115**, 7543-7588.
5. P. R. Ashton, B. Odell, M. V. Reddington, A. M. Z. Slawin, J. F. Stoddart and D. J. Williams, *Angewandte Chemie International Edition in English*, 1988, **27**, 1550-1553.
6. S. Kang, S. A. Vignon, H.-R. Tseng and J. F. Stoddart, *Chemistry – A European Journal*, 2004, **10**, 2555-2564.
7. W.-Q. Deng, A. H. Flood, J. F. Stoddart and W. A. Goddard, *Journal of the American Chemical Society*, 2005, **127**, 15994-15995.
8. S. Saha, A. H. Flood, J. F. Stoddart, S. Impellizzeri, S. Silvi, M. Venturi and A. Credi, *Journal of the American Chemical Society*, 2007, **129**, 12159-12171.
9. A. Malfait, F. Coumes, D. Fournier, G. Cooke and P. Woisel, *European Polymer Journal*, 2015, **69**, 552-558.
10. V. R. de la Rosa, P. Woisel and R. Hoogenboom, *Materials Today*, 2016, **19**, 44-55.
11. L. Sambe, V. R. de la Rosa, K. Belal, F. Stoffelbach, J. Lyskawa, F. Delattre, M. Bria, G. Cooke, R. Hoogenboom and P. Woisel, *Angewandte Chemie International Edition*, 2014, **53**, 5044-5048.
12. J. Bigot, M. Bria, S. T. Caldwell, F. Cazaux, A. Cooper, B. Charleux, G. Cooke, B. Fitzpatrick, D. Fournier, J. Lyskawa, M. Nutley, F. Stoffelbach and P. Woisel, *Chemical Communications*, 2009, **35**, 5266-5268.
13. H. Guo, D. Hourdet, A. Marcellan, F. Stoffelbach, J. Lyskawa, L. de Smet, A. Vebr, R. Hoogenboom and P. Woisel, *Chemistry – A European Journal*, 2020, **26**, 1292-1297.
14. G. Maatz, A. Maciolk and H. Ritter, *Beilstein Journal of Organic Chemistry*, 2012, **8**, 1929-1935.
15. A. F. Hirschbiel, B. V. Schmidt, P. Krolla-Sidenstein, J. P. Blinco and C. Barner-Kowollik, *Macromolecules*, 2015, **48**, 4410-4420.
16. J. F. Van Guyse, D. Bera and R. Hoogenboom, *Polymers*, 2021, **13**, 374.
17. X. Ji, J. Chen, X. Chi and F. Huang, *ACS Macro Letters*, 2014, **3**, 110-113.
18. F. D. Jochum, J. Brassinne, C.-A. Fustin and J.-F. Gohy, *Soft Matter*, 2013, **9**, 2314-2320.
19. L. Sambe, F. Stoffelbach, K. Poltorak, J. Lyskawa, A. Malfait, M. Bria, G. Cooke and P. Woisel, *Macromolecular Rapid Communications*, 2014, **35**, 498-504.
20. B. Yeniad, K. Ryskulova, D. Fournier, J. Lyskawa, G. Cooke, P. Woisel and R. Hoogenboom, *Polymer Chemistry*, 2016, **7**, 3681-3690.

21. Q. Zhang, C. Weber, U. S. Schubert and R. Hoogenboom, *Materials Horizons*, 2017, **4**, 109-116.
22. J. Seuring and S. Agarwal, *Macromolecular Rapid Communications*, 2012, **33**, 1898-1920.
23. N. Audureau, C. Veith, F. Coumes, T. P. T. Nguyen, J. Rieger and F. Stoffelbach, *Macromolecular Rapid Communications*, 2021, **42**, 2100556.

For Table of Content only

The hydrophobic interactions involved in phase separation of LCST polymers are the critical factor inducing the BBox release from the BBox/naphthalene while the host-guest complexes remain stable during phase separation of UCST polymers upon cooling.



SUPPORTING INFORMATIONS

Mechanism insights in controlling host-guest (de)complexation by thermoresponsive polymer phase transitions

Experimental section

Materials

Acrylamide (Am, $\geq 99\%$, Aldrich) and 2,2'-azobis(4-methoxy-2,4-dimethylvaleronitrile) (V-70, Wako) were used as received. 2,2'-azobis(isobutyronitrile) (AIBN, $\geq 98\%$, Aldrich) was recrystallized from methanol, *N*-Isopropylacrylamide (NIPAm, $\geq 98\%$, Aldrich) was recrystallized from *n*-hexane. *N,N*-Diethylacrylamide (DEAm, TCI-Chem) was purified by redistillation prior to synthesis. All organic solvents were analytical grade and water was purified with a Millipore system combining inverse osmosis membrane (Milli RO) and ion

exchange resins (Milli Q) for synthesis and purification. RAFT agent Naphtha-CTA and cyclobis(paraquat-*p*-phenylene) (Blue Box, abbreviated as **BBox**) were prepared as previously reported.¹ *N*-Cyanomethylacrylamide (CMAM) monomer was synthesized as previously described.²

Nuclear magnetic resonance (NMR)

For chemical analyses, ¹H NMR spectra were recorded on a Bruker 300 MHz FT-NMR spectrometer at room temperature, in D₂O or DMSO-*d*₆ and chemical shifts (δ) are given in ppm. For the host-guest complexation studies at different temperatures, ¹H NMR spectra were recorded on a Bruker Advance III HD spectrometer operating at 700 MHz, using a standard 5 mm broadband Smart Probe. The temperature control was achieved by a Bruker BCU II unit and a build in temperature control unit. Following experimental conditions were employed for the variable temperature experiments: 32 scans, 45-degree flip angle, 2.5 sec acquisition time, 2 sec relaxation delay. The analyzes were performed from the soluble state to the precipitated state. The sample was allowed to equilibrate for 10 minutes at each temperature. The chemical shifts were referred to as residual HOD peak at each temperature.

Size exclusion chromatography (SEC)

For Naphtha-PNIPAm and Naphtha-PDEAm, the SEC analyses were carried out at 35°C in THF as mobile phase at a flow rate of 1 mL·min⁻¹ using toluene as a flow marker. Polymer solution was prepared at a concentration of 5 mg·mL⁻¹ and filtered through a 0.2 μ m PTFE

membrane. The separation system was composed of three columns from Waters (Styragel HR1, Styragel HR3, Styragel HR4) coupled with Wyatt's modular differential refractive index (RI) detector. The relative number-average molar mass (\overline{M}_n), relative weight-average molar mass (\overline{M}_w) and the dispersity ($D = (\overline{M}_w/\overline{M}_n)$) were calculated from a calibration curve based on narrow polystyrene (PS) standards. For Naphtha-P(CMAM-co-Am), the SEC analysis was carried out at 60 °C in DMF (+ LiBr, 1 g·L⁻¹) as mobile phase at a flow rate of 0.8 mL·min⁻¹ using toluene as a flow marker. Polymer solution was prepared at a concentration of 5 mg·mL⁻¹ and filtered through a 0.2 µm PTFE membrane. The separation system was composed of two PSS GRAM 1000 Å columns and one PSS GRAM 30 Å coupled with a modular differential refractive index (RI) detector Viscotek 3580 from Malvern. The relative number-average molar mass (\overline{M}_n), relative weight-average molar mass (\overline{M}_w) and the dispersity ($D = (\overline{M}_w/\overline{M}_n)$) were calculated from a calibration curve based on narrow *poly(methyl methacrylate)* (PMMA) standards.

Ultraviolet-Visible Spectrometry

A Cary 3500 Scan UV-Visible spectrometer equipped with a multicell Peltier temperature controller was used. The (co)polymer solution was prepared at 10 mg·mL⁻¹ and placed in 10 mm path length quartz cells from Hellma. Absorbance spectra without and with BBox were collected at 20°C for Naphtha-PNIPAm and Naphtha-PDEAm and at 65°C for Naphtha-P(CMAM-co-Am). Turbidimetry curves were built by collecting the absorbance at 670 nm

(wavelength at which clear solutions do not absorb) with a scanning rate of 1 °C min⁻¹. The LCST-type cloud point temperatures were defined during the heating as the temperature corresponding to a transmittance of 50%. The UCST-type cloud point temperatures were defined during the cooling as the temperature corresponding to a transmittance of 50 %.

Isothermal Titration Calorimetry (ITC)

Isothermal titration calorimetry (ITC) experiments were performed at 15°C for LCST polymers and 60°C for the UCST polymer, using a nano-ITC titration calorimeter from TA Instruments with a standard sample cell volume of 1 mL, following standard procedures. Compounds were dissolved in de-ionized water and the solutions were degassed gently under vacuum before use. A 250 µL injection syringe was used to inject the Blue Box solution and the titrations were performed under stirring at 400 rpm.

Synthesis of Naphtha-PNIPAm

A solution of Naphtha-CTA (97 mg, 1.7×10^{-1} mmol), AIBN (7.0 mg, 4.1×10^{-2} mmol), NIPAm monomer (3.0 g, 26.5 mmol) in DMF (4.8 mL) was deoxygenated by bubbling nitrogen for 30 min at room temperature. The reaction flask was placed in an oil bath at 80 °C. The polymerization was allowed to proceed for 2 h under constant magnetic stirring. The solution was cooled down to room temperature and the polymer isolated by precipitation in diethyl ether. It was purified further by two consecutive precipitations from acetone into diethyl ether to obtain a pure product after drying overnight under vacuum.

Synthesis of Naphtha-PDEAm

A solution of Naphtha-CTA (89 mg, 1.5×10^{-1} mmol), AIBN (6.0 mg, 3.7×10^{-2} mmol), DEAm monomer (2.70 g, 21.2 mmol) in DMF (20 mL) was deoxygenated by bubbling nitrogen for 30 min at room temperature. The reaction flask was placed in an oil bath at 70 °C. The polymerization was allowed to proceed for 3 h under constant magnetic stirring. Then, the solution was cooled down to room temperature and the polymer isolated by precipitation in *n*-hexane. It was purified further by two successive precipitations from acetone into *n*-hexane to obtain a pure product after drying overnight under vacuum.

Synthesis of Naphtha-P(CMAm-*co*-Am)

A solution of Naphtha-CTA (31.8 mg, 5.4×10^{-2} mmol), V-70 (8.3 mg, 2.7×10^{-2} mmol), CMAm monomer (0.608 g, 5.5 mmol) and Am monomer (0.169 g, 2.4 mmol) in DMF (3 mL) was deoxygenated by bubbling argon for 15 min at 5 °C (cold water bath). The reaction flask was placed in an oil bath at 35 °C. The polymerization was allowed to proceed for 3 h under constant magnetic stirring. The solution was cooled down to room temperature and the polymer isolated by precipitation in chloroform, dried under vacuum, solubilized in water, purified by dialysis against water for 2 days (membrane cut off of 1 kDa) and finally freeze-dried.

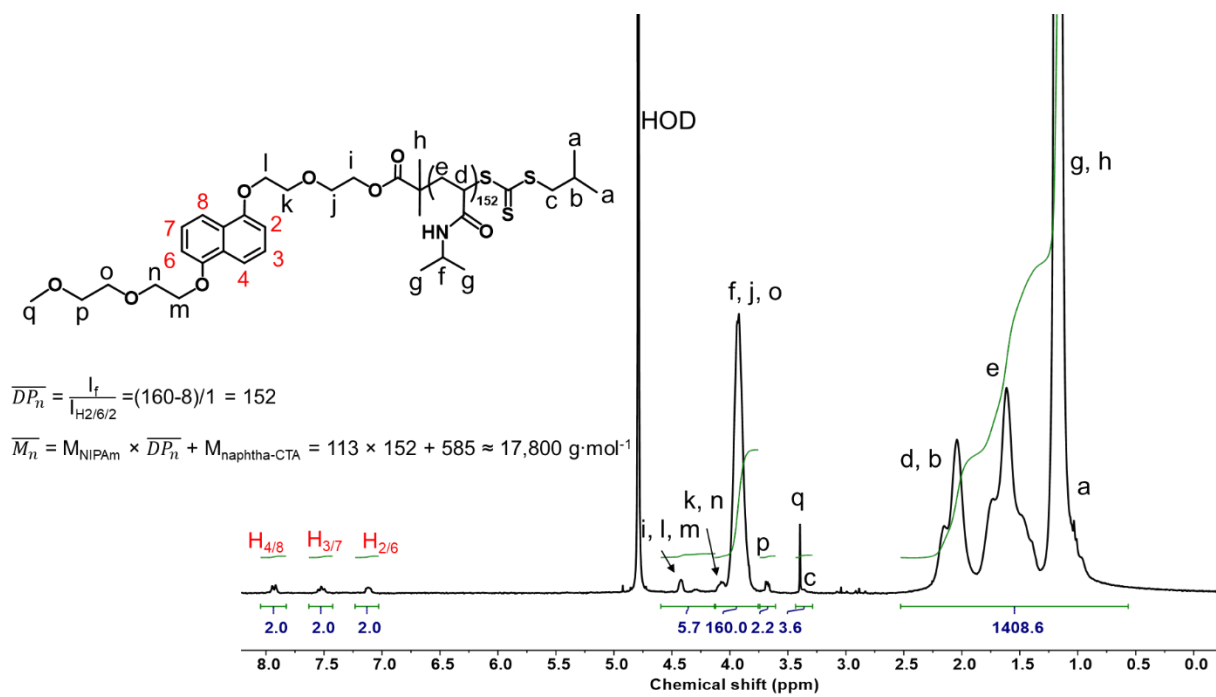


Fig. S1. ¹H NMR spectrum of Naphtha-PNIPAm₁₅₂ in D₂O.

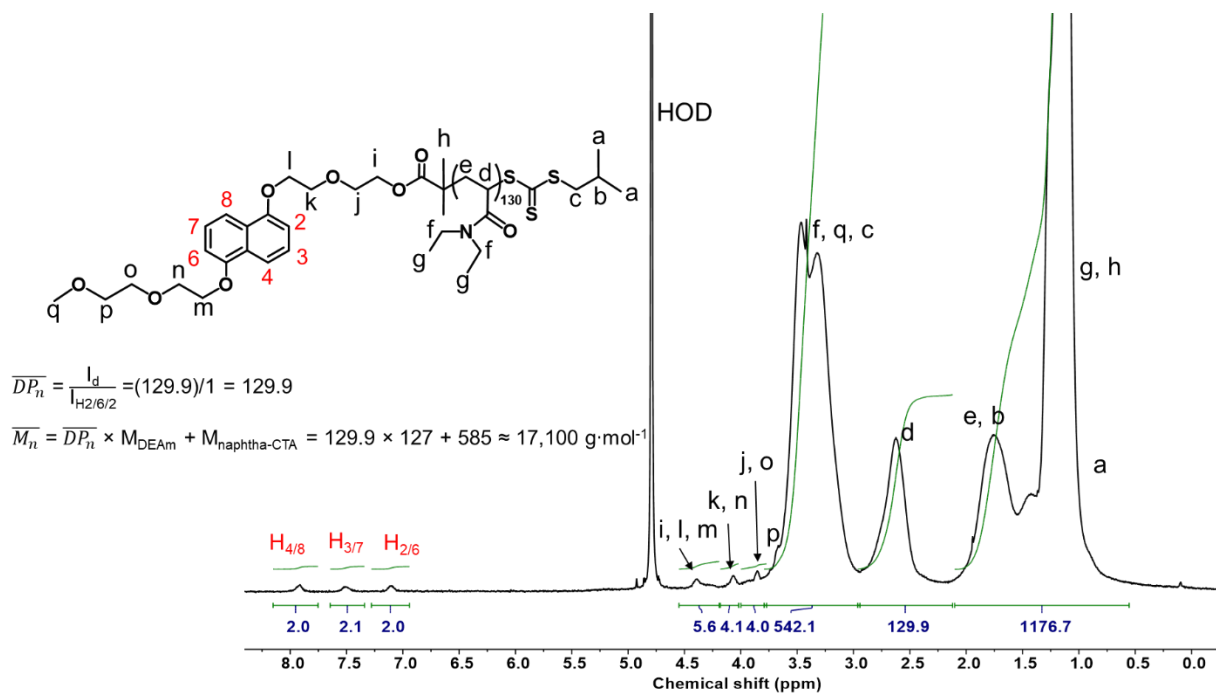


Fig. S2. ¹H NMR spectrum of Naphtha-PDEAm₁₃₀ in D₂O.

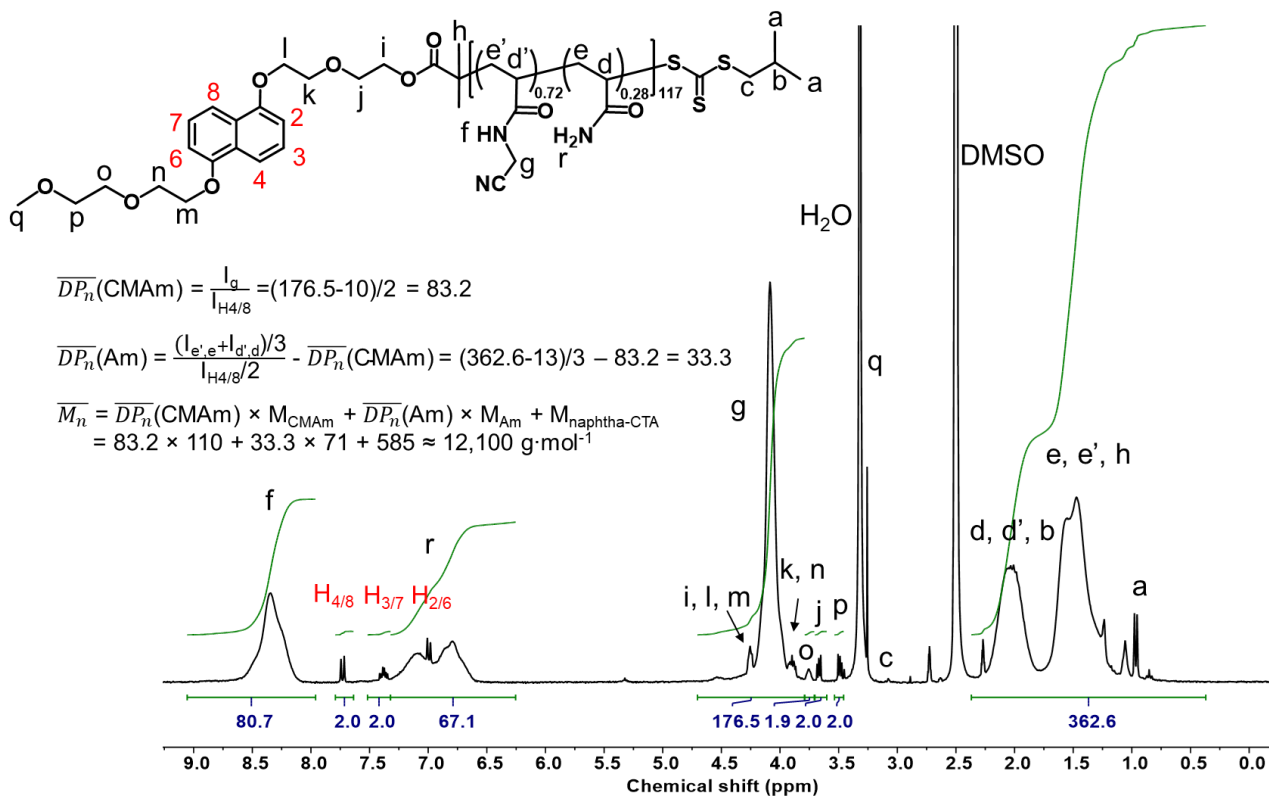


Fig. S3. ^1H NMR spectrum of Naphtha-P(CMAm_{0.72}-co-Am_{0.28})₁₁₇ in DMSO-*d*₆.

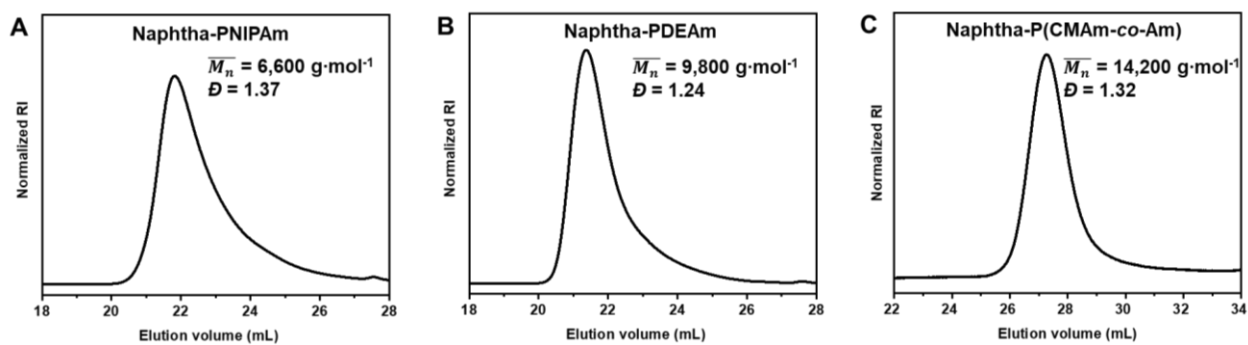


Fig. S4. Size-exclusion chromatography profiles of A) Naphtha-PNIPAm, B) Naphtha-PDEAm and C)

Naphtha-P(CMAm-co-Am).

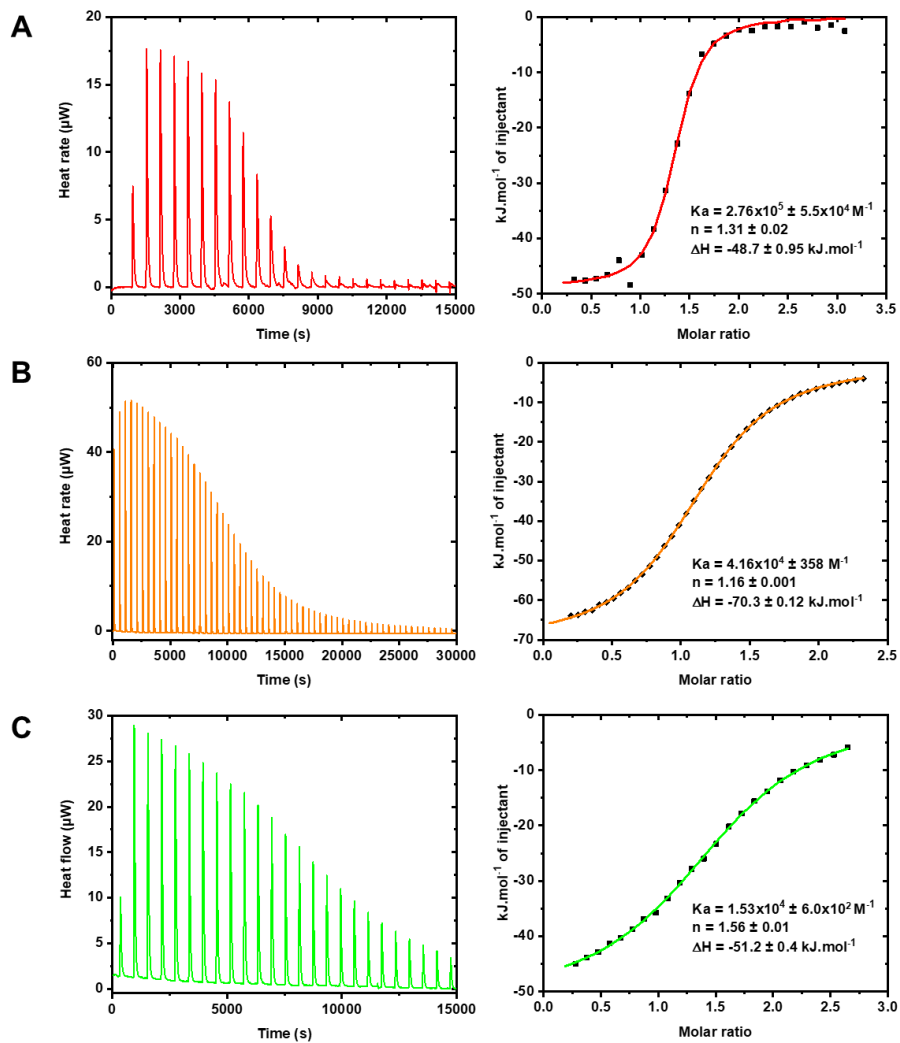


Fig. S5. Isothermal titration calorimetry data for the addition of aliquots of **BBox** to A) **Naphtha-PNIPAm** polymer (recorded in H_2O at $15\text{ }^\circ\text{C}$), B) **Naphtha-PDEAm** polymer (recorded in H_2O at $15\text{ }^\circ\text{C}$), C) **Naphtha-P(CMAm-co-Am)** (recorded in H_2O at $60\text{ }^\circ\text{C}$).

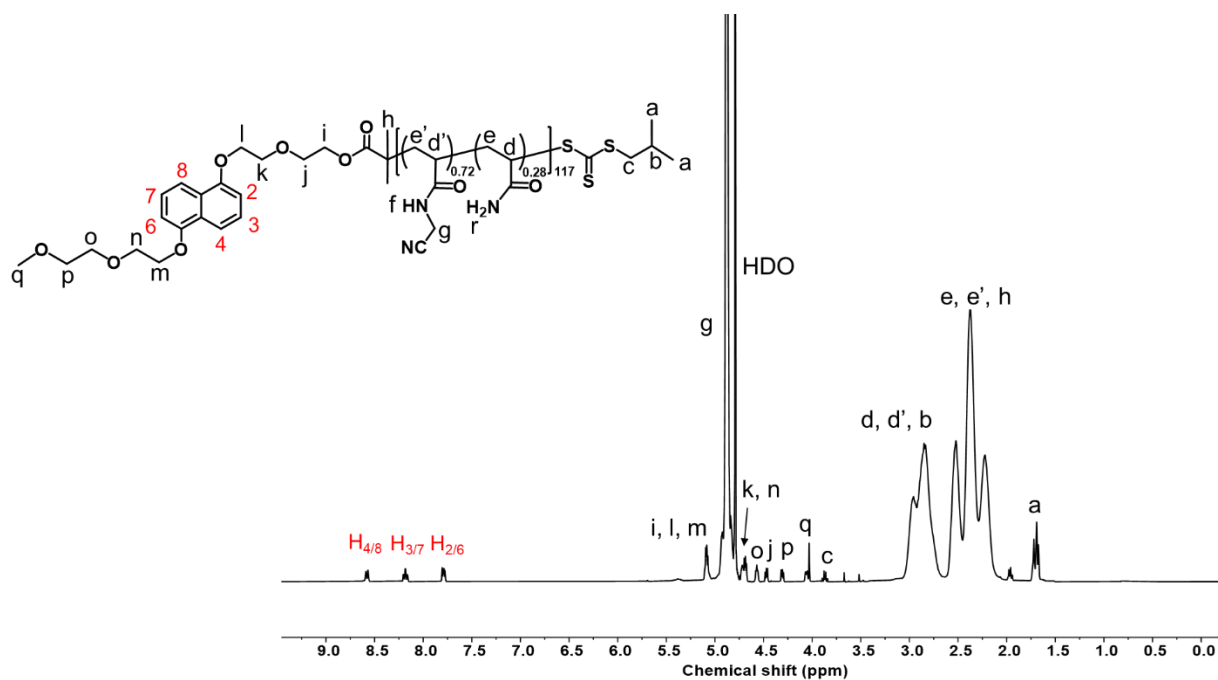


Fig. S6. ^1H NMR spectrum of **Naphtha-P(CMAM_{0.72}-co-Am_{0.28})₁₁₇** in D_2O at $90\text{ }^\circ\text{C}$.

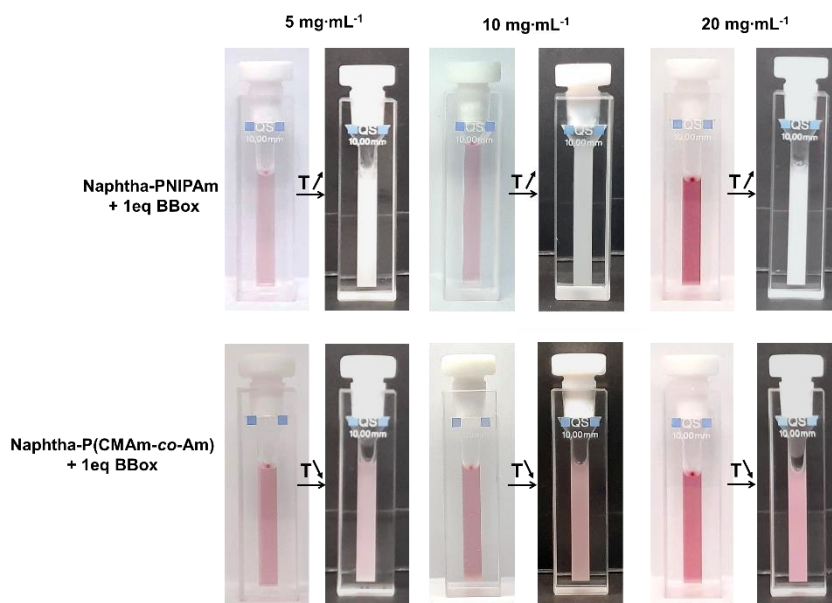


Fig.S7. Photographs of **Naphtha-PNIPAm** (top) and **Naphtha-P(CMAM-co-Am)** (bottom) in pure water at $5\text{ mg}\cdot\text{mL}^{-1}$, $10\text{ mg}\cdot\text{mL}^{-1}$ and $20\text{ mg}\cdot\text{mL}^{-1}$ with 1 equivalent of BBox at different temperatures.

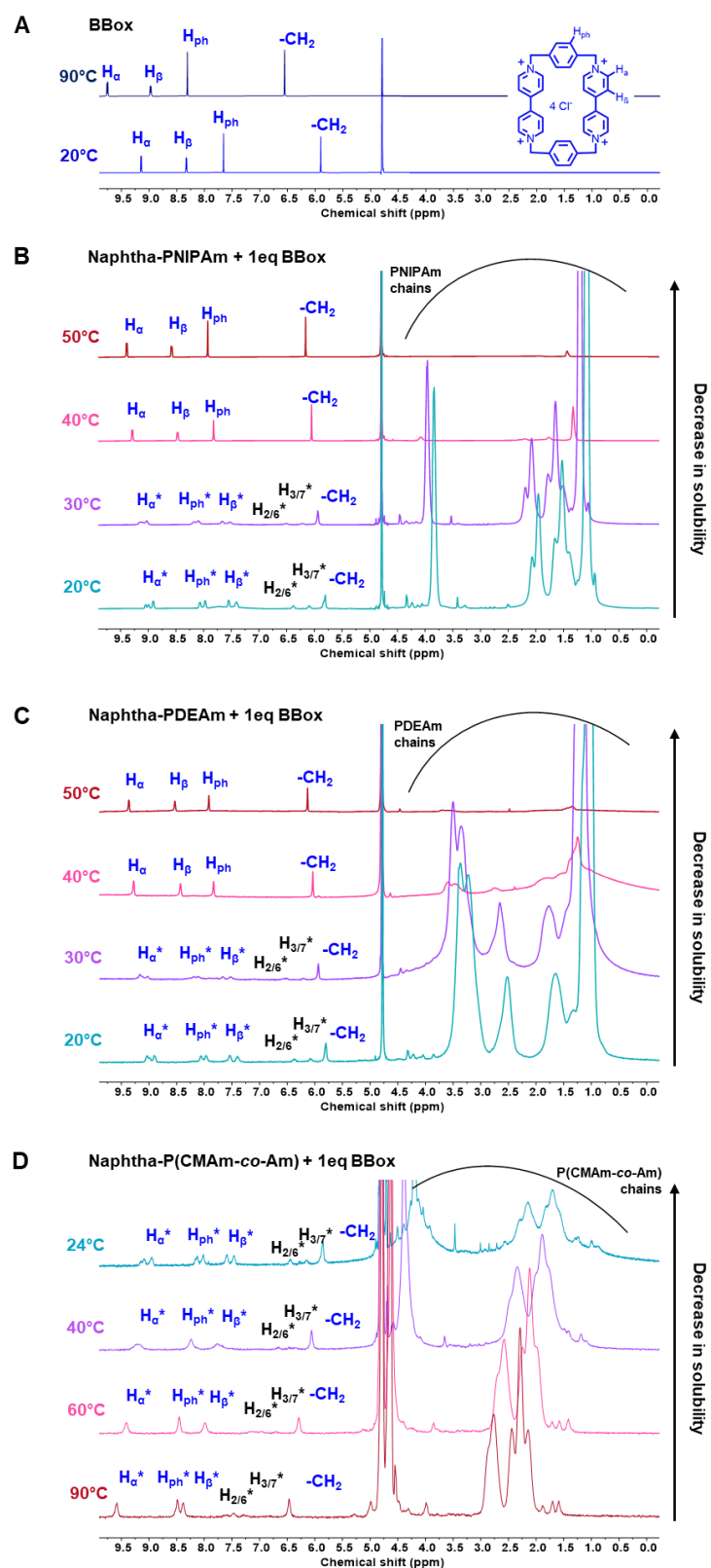


Fig. S8. ^1H NMR spectra in D_2O of A) **BBox** alone at 20 and 90 °C (for comparison), B) **Naphtha-PNIPAm** polymer with 1 eq of **BBox** at 20, 30, 40 and 50 °C, C) **Naphtha-PDEAm** polymer with 1 eq of **BBox** at 20, 30, 40 and 50 °C, D) **Naphtha-P(CMAM-co-Am)** with 1 eq of **BBox** at 90, 60, 40 and 24 °C. The protons

H* denote complexed protons from naphthalene moieties and **BBox**.

References

1. J. Bigot, M. Bria, S. T. Caldwell, F. Cazaux, A. Cooper, B. Charleux, G. Cooke, B. Fitzpatrick, D. Fournier, J. Lyskawa, M. Nutley, F. Stoffelbach and P. Woisel, *Chemical Communications*, 2009, **35**, 5266-5268.
2. N. Audureau, C. Veith, F. Coumes, T. P. T. Nguyen, J. Rieger and F. Stoffelbach, *Macromolecular Rapid Communications*, 2021, **42**, 2100556.